

A novel copper complex supported on magnetic reduced graphene oxide: an efficient and green nanocatalyst for the synthesis of 1-amidoalkyl-2-naphthol derivatives

M. Kooti · M. Karimi · E. Nasiri

Received: 25 July 2017 / Accepted: 15 December 2017 / Published online: 17 January 2018
© Springer Science+Business Media B.V., part of Springer Nature 2018

Abstract A new Cu(II) complex supported on magnetic reduced graphene oxide was prepared and characterized by various techniques, such as FT-IR, XRD, SEM, EDX, TEM, TGA, BET, ICP, and VSM. The synthesized nanocomposite, which has size distribution of 25–30 nm, was employed as catalyst in one-pot synthesis of 1-amidoalkyl-2-naphthols via three-component condensation reaction of amides, aromatic aldehydes, and 2-naphthol, under solvent-free conditions. The introduced catalysis procedure for the synthesis of 1-amidoalkyl-2-naphthol derivatives offers several advantages namely, short reaction times, high yields, facile recyclability, and cost effectiveness.

Keywords Cu(II) complex · 1-Amidoalkyl-2-naphthol · Reduced graphene oxide · Cobalt ferrite · Nanocatalyst · Multicomponent reactions · Environmental effect

Introduction

Substantial research attention has been drawn to the newly emerged multi-component reactions (MCRs) in recent years (Safari et al. 2014; Rakhtshah and

Electronic supplementary material The online version of this article (<https://doi.org/10.1007/s11051-017-4107-0>) contains supplementary material, which is available to authorized users.

M. Kooti (✉) · M. Karimi · E. Nasiri
Department of Chemistry, ShahidChamran University of Ahvaz,
Ahvaz, Iran
e-mail: m_kooti@scu.ac.ir

Salehzadeh 2016; Tayebie et al. 2014). This is because MCRs can offer the possibility of obtaining diverse and complex organic molecules from simple building blocks in a single step (Nasr Esfahani et al. 2016; Gupta et al. 2016). Using MCRs in organic synthesis, especially when they are performed under solvent-free conditions sometimes also called as zipper reactions, can practically minimize the reaction times, unwanted by-products, energy, and environmental pollutions (Zhang et al. 2010). The newly developed MCRs, therefore, have been frequently used for the synthesis of some valuable compounds such as 1-amidoalkyl-2-naphthols. There are many reasons for the importance of 1-amidoalkyl-2-naphthol derivatives, including their potentially useful biological and pharmacological properties (Maleki et al. 2016; Moghanian et al. 2014; Taghrir et al. 2016; Kiasat et al. 2013). 1-Amidoalkyl-2-naphthols are commonly prepared via condensation reaction of aliphatic and/or aromatic aldehydes, 2-naphthol, and acetonitrile or amides in the presence of heterogeneous acid catalyst. Several catalysts, either Lewis or Brønsted acids, have been used to initiate this condensation reaction, such as graphene oxide (Gupta et al. 2016), sulfamic acid (Shaterian et al. 2008a, b), FeCl₃@SiO₂ (Shaterian et al. 2008a, b), heteropoly acids (Khabazzadeh et al. 2009), Fe(HSO₄)₃ (Shaterian et al. 2008a, b), K₅CoW₁₂O₄₀·3H₂O (Nagarapu et al. 2007), and Cu(II) acetylacetonate (Khairnar et al. 2016).

A desirable catalyst in any organic reaction has to be environmentally benign, easily recoverable, cost effective, and highly efficient at mild conditions. Most of the so far used catalysts for the synthesis of

1-amidoalkyl-2-naphthols do not meet all these clear-cut criteria. They suffer from some drawbacks, such as long reaction times, low product yields, the use of strongly acidic media, toxic or corrosive reagents, and complex equipment or experimental conditions. Therefore, designing of new catalysis system for the preparation of medicinally important amidoalkyl-2-naphthols, which has the least disadvantages, still remains a challenge (Nandi et al. 2009; Nagarapu et al. 2007; Kantevari et al. 2007; Singha et al. 2015; Zhu et al. 2012; Chen et al. 2013).

On the other hand, graphene, one of the thinnest materials with two-dimensional carbon sheet structure, has inspired enormous interest in diverse fields including catalytic chemistry. The extraordinary and unique properties of graphene make it one of the most favorable material for wide interesting applications (Sheshmani

and Amini 2013; Georgakilas et al. 2012; Su et al. 2013; Allen et al. 2009; Guo et al. 2012; Gemeay et al. 2017; Rayati et al. 2017; Li et al. 2013; Rondinone et al. 1999; Chandekar and Kant 2017; Kumar et al. 2013). Moreover, combining of graphene with a magnetic material, such as CoFe_2O_4 , will provide an excellent means for separation of graphene composites via magnetic decantation as well as reducing the agglomeration tendency of graphene sheets (Yan et al. 2010; Xiong et al. 2014; Rakjumar and Rao 2008; Sofia et al. 2009; Zhang et al. 2009). Magnetic nanoparticles (MNPs) deposited on the surface of graphene sheets can provide a suitable inorganic support for designing and constructing novel nanocatalysts. The fascinating feature of nanocatalysts containing MNPs is their ease of separation from the reaction media by applying an external magnet, which eliminates the need for tedious filtration or centrifugation

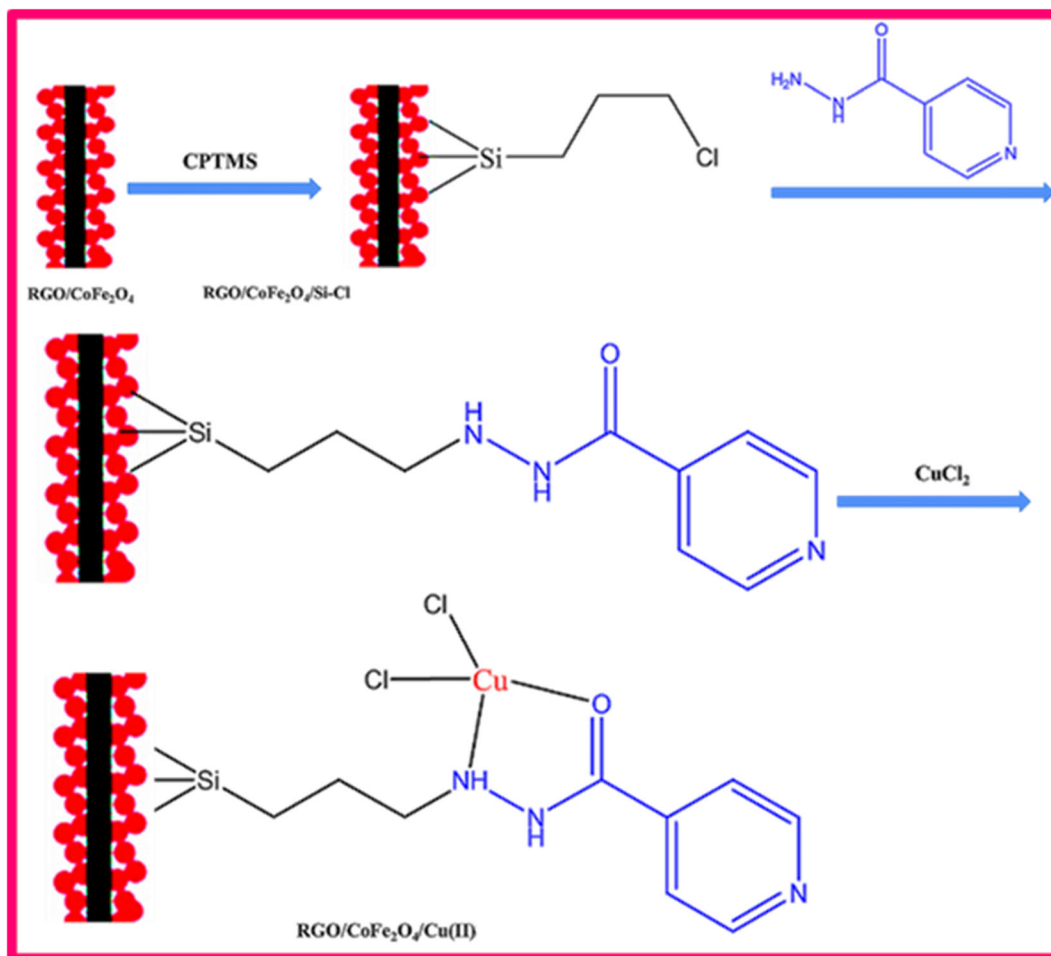


Fig. 1 Schematic representation of step-by-step preparation of $\text{RGO/CoFe}_2\text{O}_4@\text{Cu(II)}$ nanocatalyst

processes. Another benefit of the MNPs presence in a solid catalyst is providing the required high surface area for desired functionalization (Dupont et al. 2002; Virtanen et al. 2010; Hosseini and Asadnia 2012; Jiang et al. 2009; Zheng et al. 2009; Polshettiwar et al. 2011; Lee et al. 2007; Majidi et al. 2006).

We herein report the synthesis of a new composite consisted of Cu(II) complex immobilized on magnetized reduced graphene oxide (RGO) and its application as catalyst for the synthesis of 1-amidoalkyl-2-naphthols. Three-component one-pot condensations of aldehydes, 2-naphthol, and amides were performed in the presence of this prepared nanocatalyst, under solvent-free conditions to give 1-amidoalkyl-2-naphthol derivatives. The synthesized composite, in which the Cu(II) center acts as Lewis acid, exhibited high catalytic activity in these condensation reactions. To the best of our knowledge, this is the first Cu(II) complex supported on magnetic RGO which is used as catalyst for the preparation of 1-amidoalkyl-2-naphthol derivatives.

Experimental

Graphene oxide (GO) was prepared and purified by the Hummers' method (Rakjumar and Rao 2008) and converted to RGO using sodium borohydride (NaBH_4) as reducing agent (Sofia et al. 2009). The RGO/ CoFe_2O_4 composite was synthesized by dispersing of 0.4 g of RGO into 100 mL of deionized water with sonication for 2 h, and to this suspension, 4.04 g of $\text{Fe}(\text{NO}_3)_3 \cdot 9\text{H}_2\text{O}$ and 1.45 g of $\text{Co}(\text{NO}_3)_2 \cdot 6\text{H}_2\text{O}$, dissolved in 25 mL of water, was added. After adjusting the pH of the mixture at 11–12 with 2 M NaOH and addition of 1.0 g of polyvinylpyrrolidone (PVP), as surfactant, it was heated at 80 °C for 3 h under continuous magnetic stirring. The obtained nanocomposite was collected by applying a permanent magnet and washed with hot water-ethanol and finely powdered after being dried in an oven at 60 °C for 24 h. In the next step, 1.0 g of RGO/ CoFe_2O_4 composite was dispersed in 50 mL of dry toluene using an ultrasonic bath to produce a

Fig. 2 FT-IR spectra of RGO/ CoFe_2O_4 (A), RGO/ CoFe_2O_4 @Si-Cl (B), RGO/ CoFe_2O_4 @Si-4-Pyridin carbohydrazide (C), and RGO/ CoFe_2O_4 @Cu(II) (D)

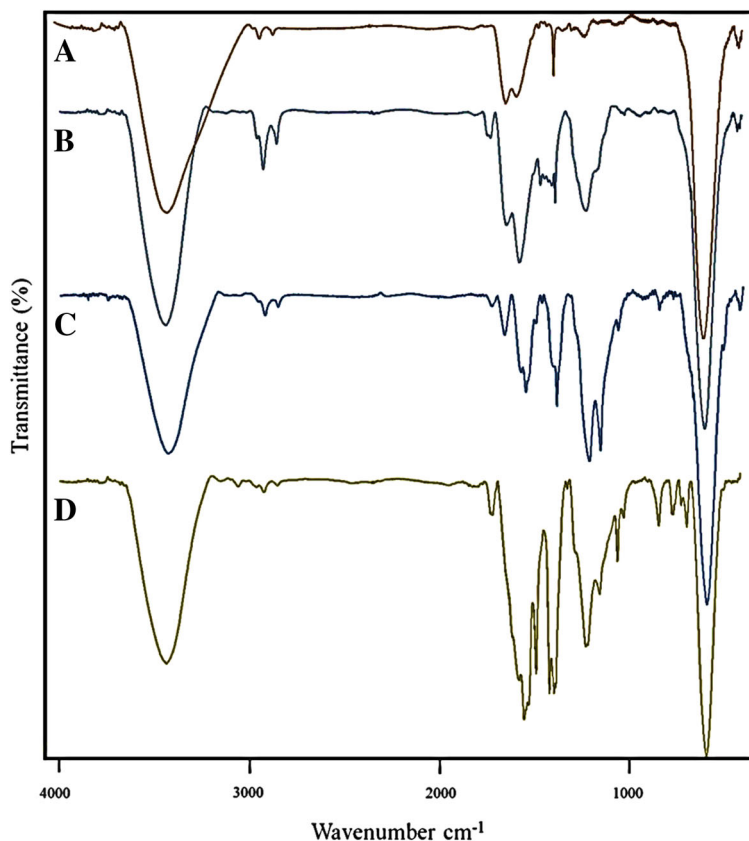
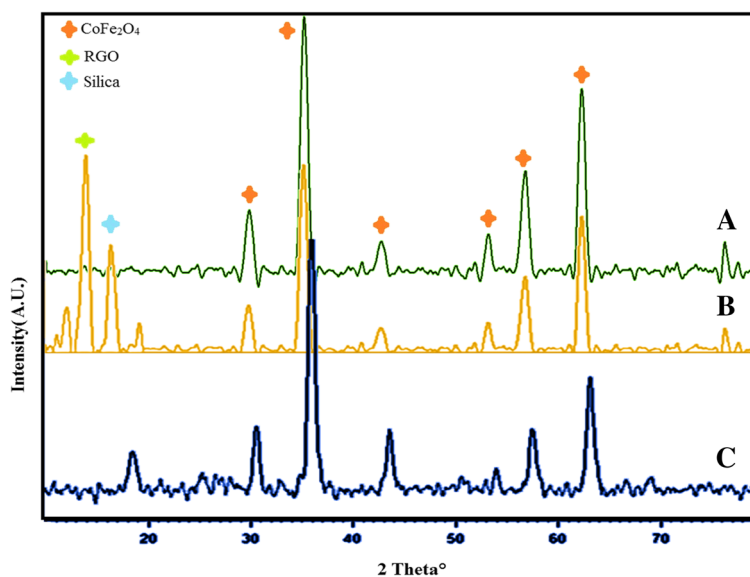


Fig. 3 PXRD patterns of CoFe_2O_4 (A), RGO/ CoFe_2O_4 @Si-Cl (B), and RGO/ CoFe_2O_4 @Cu(II) (C)



uniform suspension, and to this solution, 1.0 mL (5.5 mmol) of 3-chloropropyltrimethoxysilane (CPTMS) was added. The mixture was then stirred for 48 h at 80 °C. Finally, the obtained solid product was washed with toluene and dried in an oven to yield CPTMS functionalized RGO/ CoFe_2O_4 (designated as RGO/ CoFe_2O_4 /Si-Cl). The Cu(II) complex was immobilized on the surface of RGO/ CoFe_2O_4 /Si-Cl as follows: 0.75 g (5.5 mmol) of 4-pyridinecarboxylic acid hydrazide, as ligand (Patel et al. 2013), was added to 1.0 g of well-dispersed RGO/ CoFe_2O_4 /Si-Cl in 40 mL of ethanol and the mixture was stirred for 24 h at 60 °C. The resulting solid was mixed with $\text{CuCl}_2 \cdot 2\text{H}_2\text{O}$ (0.93 g, 5.5 mmol) in 40 mL of ethanol and stirred for 24 h at 60 °C. The obtained product which is Cu(II) complex anchored

on the surface of RGO/ CoFe_2O_4 (designated as RGO/ CoFe_2O_4 @Cu(II)) was washed with 60 mL of ethanol (three times each time with 20 mL) and dried in an oven at 60 °C for 24 h.

Synthesis of 1-amidoalkyl naphthols catalyzed by RGO/ CoFe_2O_4 @Cu(II)

Of RGO/ CoFe_2O_4 @Cu(II), as nanocatalyst, 0.03 g was added to a mixture of 2-naphthol (1 mmol), aldehyde (1 mmol), and amide/urea (1.2 mmol). The mixture was magnetically stirred under solvent-free conditions in an oil bath at 120 °C for a certain period of time. The reaction was stopped when the TLC (hexane/ethyl acetate, 2:5) indicated complete consumption of the starting substrates. After completion, the resultant solid product

Fig. 4 SEM (a) and TEM (b) images of RGO/ CoFe_2O_4 @Cu(II)

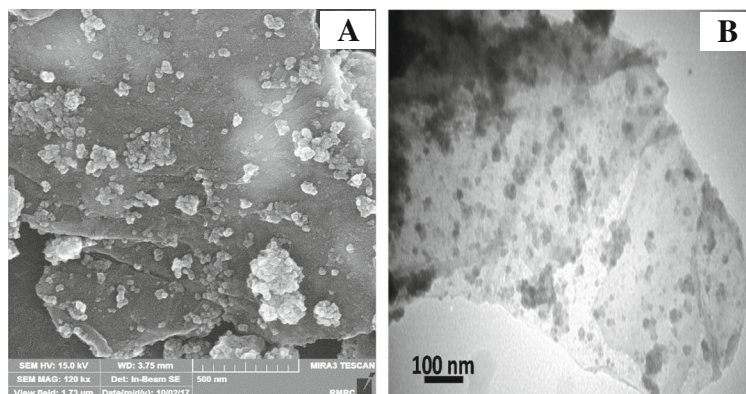


Fig. 5 EDX spectrum of **a** RGO/
CoFe₂O₄@Si-4-Pyridin
carbohydrazide; **b** RGO/
CoFe₂O₄@Cu(II)

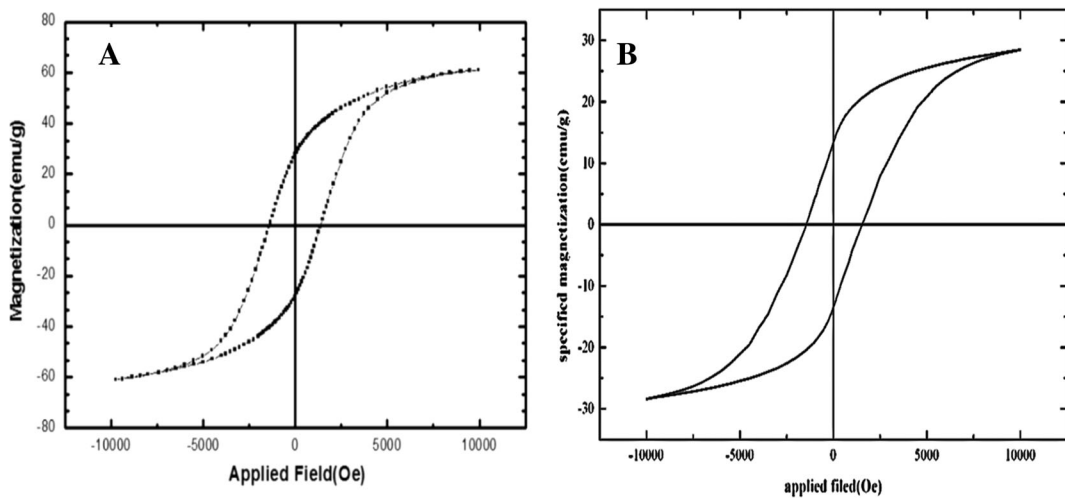
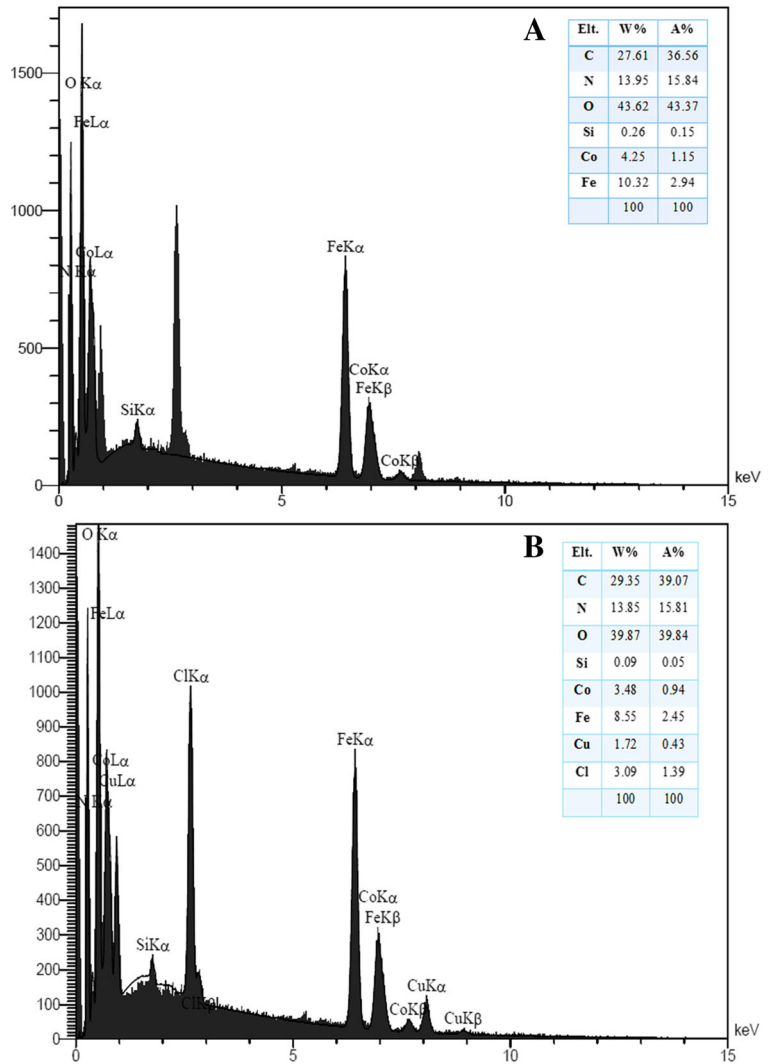
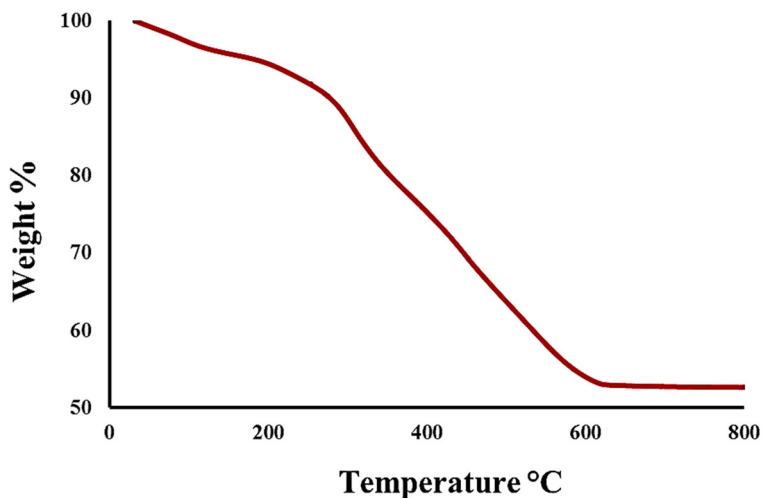


Fig. 6 Hysteresis loops of CoFe₂O₄ (**a**) and RGO/CoFe₂O₄@Cu(II) (**b**)

Fig. 7 The TGA thermogram of RGO/CoFe₂O₄@Cu(II)



was washed with hot ethanol and the nanocatalyst was separated by an external magnet and reused as such in new experiment. The obtained solid product of 1-amidoalkyl-2-naphthol was purified by recrystallization in aqueous ethanol solution to give pure product which was identified by comparison of their spectroscopic and physical data with those reported for known samples. The sequential procedure for the synthesis of RGO/CoFe₂O₄@Cu(II) nanocatalyst is presented in Fig. 1.

Results and discussion

The Cu(II) complex supported on RGO/CoFe₂O₄, as a heterogeneous nanocatalyst, was characterized with FT-IR, XRD, SEM, EDX, TEM, BET, TGA, and VSM techniques.

In order to confirm the presence of the copper complex on the surface of RGO/CoFe₂O₄, FT-IR spectra of the as-synthesized materials were obtained and are

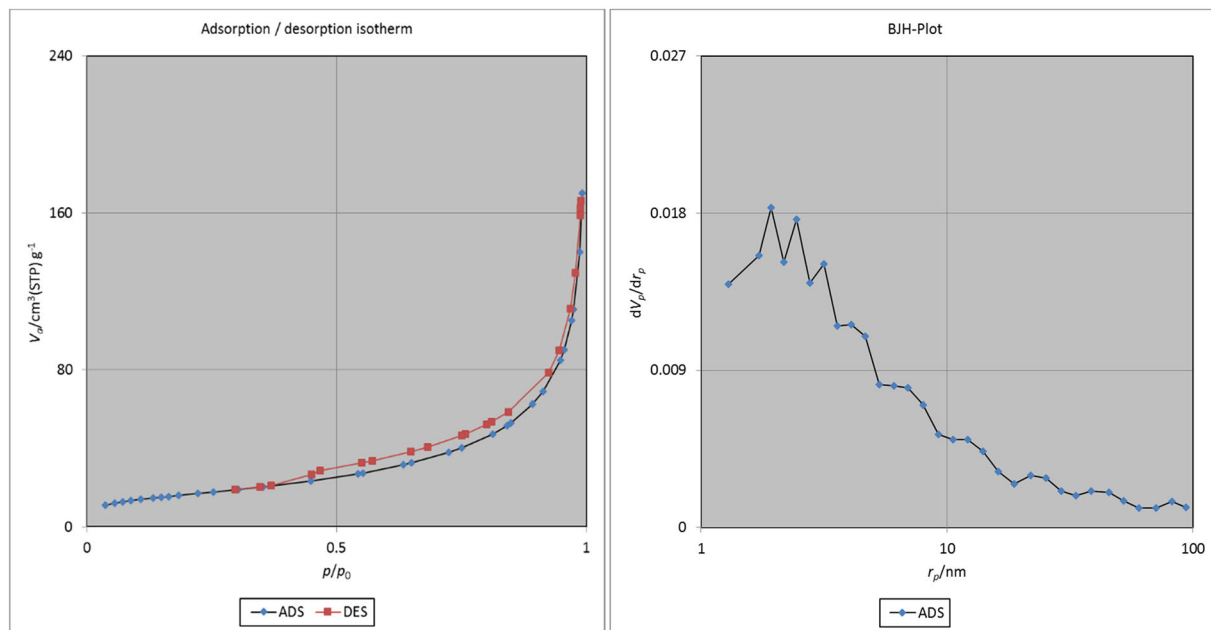


Fig. 8 N₂ adsorption/desorption isotherm and BJH-Plot of RGO/CoFe₂O₄@Cu(II)

Table 1 Effect of different catalysts, amount of catalyst, and temperature range on the preparation of amidoalkyl naphthol derivatives under solvent-free conditions ^a

Entry	Catalyst	Temperature (°C)	Time (min)	Yield %
1	RGO	120	60	40
2	CoFe ₂ O ₄	120	60	30
3	RGO/CoFe ₂ O ₄	120	60	42
4	RGO/CoFe ₂ O ₄ -Si-NH ₂	120	60	40
5	Complex (15 mg)	120	60	90
6	Catalyst (15 mg)	120	60	82
7	Catalyst (15 mg)	100	60	82
8	Catalyst (15 mg)	100	35	80
9 ^b	Catalyst (30 mg)	100	35	90

^aReaction conditions: benzaldehyde (1 mmol), 2-naphthol (1 mmol), acetamide (1.2 mmol), catalyst (15 mg). ^bcatalyst (30 mg)

shown in Fig. 2. The broad band at about 3420–3480 cm⁻¹ was assigned to O-H stretching vibration in all the synthesized compounds. Comparison the spectra of RGO/CoFe₂O₄ and RGO/CoFe₂O₄@Si-Cl in Fig. 2A and B reveals an additional strong band at 1000–1200 cm⁻¹ corresponding to the characteristic absorption of Si-O bonds in the latter composite. In the FT-IR spectrum of the RGO/CoFe₂O₄@Cu(II), the C=O stretching vibration has shifted to lower frequency (1721 cm⁻¹) after coordination of the ligand to copper metal (Fig. 2D). In all these spectra, peaks at about 595 and 421 cm⁻¹ were observed which are attributed to the Fe³⁺-O stretching vibrations of cobalt ferrite.

Figure 3 displays the PXRD patterns of CoFe₂O₄, RGO/CoFe₂O₄@Si-Cl, and RGO/CoFe₂O₄@Cu(II) nano materials. The PXRD pattern of CoFe₂O₄ (Fig. 3A) shows peaks at 2θ = 30°, 35°, 43°, 54°, 57°, and 63° expected for spinel cubic structure and all these peaks are seen in the PXRD patterns of other synthesized samples (Fig. 3B, C). This indicates that the crystallinity and morphology of CoFe₂O₄ are preserved during the grafting process. In the PXRD pattern of RGO/CoFe₂O₄@Si-Cl, peaks at 2θ = 14° and 2θ = 17° are also observed which can be assigned to RGO and silica components, respectively (Sahoo et al. 2013; Tang et al. 2012; Chang et al. 2013). The slight shift observed for these two peaks is probably due to their interactions with magnetic nanoparticles core. The crystallite size of pure CoFe₂O₄ was 25 nm as estimated by using the well-known Debye-Scherrer formula but increased to 45 nm in the final nanocatalyst.

The SEM and TEM images of RGO/CoFe₂O₄@Cu(II) are depicted in Fig. 4. The CoFe₂O₄ nanoparticles, which are well-resolved with almost spherical shapes, anchored with the copper complex can be clearly seen on the surface of RGO (Fig. 4a). Also the transmission electron microscopy (TEM) image of the as-prepared RGO/CoFe₂O₄@Cu(II) (Fig. 4b) clearly shows that CoFe₂O₄@Cu(II) on the surface of RGO has almost spherical-shaped morphology. The image indicates that CoFe₂O₄@Cu(II) (dark spots) was grafted on RGO, and the particles exhibit size distribution of 25–30 nm.

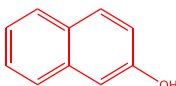
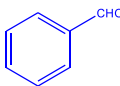
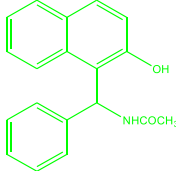
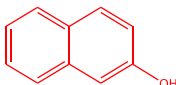
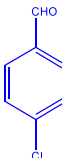
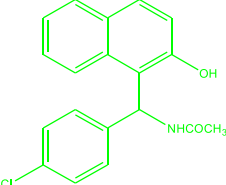
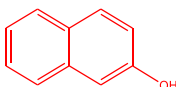
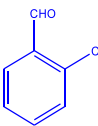
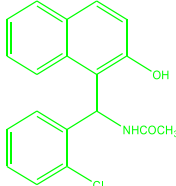
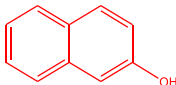
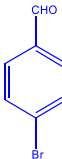
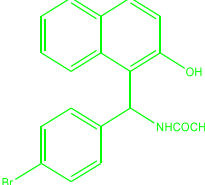
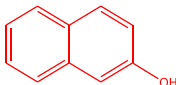
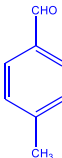
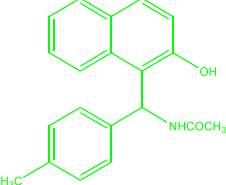
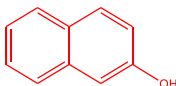
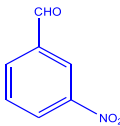
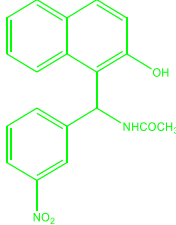
The composition of the as-fabricated RGO/CoFe₂O₄@Cu(II) nanocomposite was further affirmed by EDX analysis. The EDX spectrum of this composite is shown in Fig. 5 which indicates the presence of copper, as well as other elements such as C, O, N, Cl, and Si existed in the composite. The copper content of the complex supported on RGO/CoFe₂O₄ was also measured by ICP analysis and was found to be about 1.7%. The chloride content of RGO/CoFe₂O₄@Cu(II) was determined by potentiometric titration with silver nitrate. The amount of Cl in this composite was found to be about 2.06% and the potentiometric titration curve is shown in Fig. S2. According to the results obtained from ICP measurement and potentiometric titration, the Cu/Cl mole ratio of the composite is approximately 1:2.

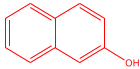
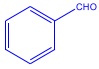
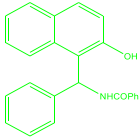
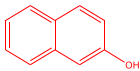
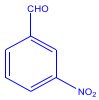
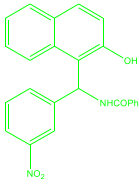
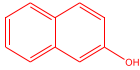

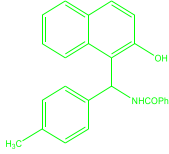
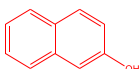
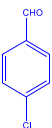
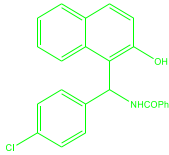
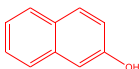
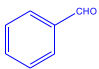
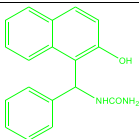
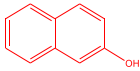

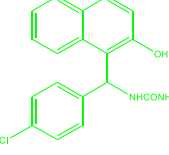
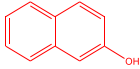
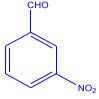
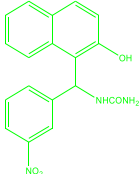
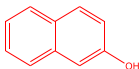

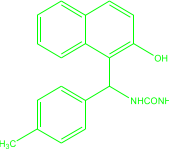
The magnetic properties of CoFe₂O₄ and RGO/CoFe₂O₄@Cu(II) were studied by a vibrating sample magnetometer (VSM), and the hysteresis loops are shown in Fig. 6. The VSM curve for RGO/CoFe₂O₄@Cu(II) nanocomposite shows that the value of saturation magnetization (M_s) is 28.5 emu g⁻¹ which is much less than the M_s value of pure CoFe₂O₄ (61 emu g⁻¹). The decrease of M_s may be due to the entrapment of CoFe₂O₄ NPs with the nonmagnetic components including silica and the copper complex. The magnetization of the RGO/CoFe₂O₄@Cu(II) composite, however, is still sufficiently high to ensure its separation and manipulation under an

Table 2 Effect of solvent on the synthesis of amidoalkyl naphthol derivatives

Entry	Solvent	Temperature(°C)	Time(min)	Yield %
1	CH ₃ CN	80	120	70
2	EtOH	75	120	60
3	CH ₂ Cl ₂	25	120	55
4	CHCl ₃	60	120	55
5	n- Hexane	25	120	50

Table 3 Three-component synthesis of amidoalkynaphthol derivatives using 0.03 g of nanocatalyst^a

Entry	Aldehyde	Amides	Product ^a	Time (min)	Yield% ^b	M.P. ^c
1				35	90	240-242 ^[4]
2				30	91	228-230 ^[4]
3				25	90	204-206 ^[4]
4				30	92	225-227 ^[6]
5				35	90	213-215 ^[8]
6				30	91	240-242 ^[4]

7			PhCONH ₂		30	90	234-236 ^[4]
8			PhCONH ₂		30	91	239-241 ^[4]
9			PhCONH ₂		35	88	208-210 ^[3]
10			PhCONH ₂		30	89	176-178 ^[4]
11			NH ₂ CONH ₂		40	87	176-178 ^[4]
12			NH ₂ CONH ₂		40	88	171-173 ^[4]
13			NH ₂ CONH ₂		40	86	186-188 ^[4]
14			NH ₂ CONH ₂		45	85	202-203

^a Reaction conditions: aldehyde (1 mmol), 2-naphthol (1 mmol), amide derivatives (1.2 mmol), 100 °C, solvent-free

^b Isolated yield

^c All compounds were identified by IR and melting point, and some compounds with ¹HNMR and results were compared to previous articles

Table 4 Comparison of efficiency of the RGO/CoFe₂O₄@Cu(II) with other catalysts

Entry	Catalyst	Solvent	Temp. °C	Time (h)	Yield%	Ref.
1	K ₂ CoW ₁₂ O ₄₀ ·3H ₂ O	–	125	3	78	Nagarapu et al. 2007
2	Iodine	–	125	5	81	Shaterian et al. 2008a
3	Sulfamoc acid	DCE	rt	7	82	Nagawade and Shinde 2007
4	Ce(SO ₄)	MeCN	70	36	72	Selvam and Perumal 2006
5	Molybdo phosphoric acid	–	65	3.5	94	Jiang et al. 2008
6	Thiamin HCl	EtOH	80	4	88	Shaterian and Yarahmadi 2008
7	NiFe ₂ O ₄ @MCM-Cl-SO ₃ H	–	100	60	92	Cai et al. 2014
8	RGO/CoFe ₂ O ₄ @Cu(II)	–	120	35	90	This work

external magnetic field.

The as-fabricated RGO/CoFe₂O₄@Cu(II) was also studied by thermogravimetric analysis and its TGA curve is given in Fig. 7. A total weight loss of 47% for the nanocatalyst was observed on heating to 600 °C. This study has been performed at temperature range of 60–1000 °C in air atmosphere. Degassing and solvent evaporation at low temperatures accounts for approximately 4% of the weight loss. The second stage is from 120 to 280 °C with a weight loss of 6%, is due to the release of the organic ligand in the Cu(II) complex. The main weight loss which occurs at temperatures from 280 to 450 °C corresponds to the combustion of residue organic ligands as well as decomposition of the composite (37%). DTA analysis of RGO/CoFe₂O₄@Cu(II) is shown in Fig. S1.

Nitrogen adsorption/desorption is a common method for characterization of mesoporous materials which provides information about the specific surface area, average pore diameter, and pore volume. N₂ adsorption-desorption isotherm and BJH pore plot of the as-prepared nanocatalyst are shown in Fig. 8. The BET surface area, pore volume, and pore diameter of RGO/CoFe₂O₄@Cu(II) are found to be 60.011 m² g⁻¹, 0.25 cm³, and 16.16 nm, respectively. The observed isotherm for RGO/CoFe₂O₄@Cu(II) corresponds to type(III)adsorption isotherm, which can also explain the formation of multilayer structure for the nanocomposite.

Evaluation of catalytic activity of RGO/CoFe₂O₄@Cu(II)

The capability of RGO/CoFe₂O₄@Cu(II) nanocomposite as a heterogeneous catalyst was evaluated in the synthesis of 1-amidoalkyl-2-naphthol derivatives. To

find optimized conditions for the reaction, various parameters, including catalyst dose, type of solvent, and different temperatures, were probed. The model reaction, condensation of benzaldehyde with 2-naphthol and acetamide, was checked with two different amounts of nanocatalyst (0.015 and 0.03 g) and better result was obtained with 0.03 g dose of catalyst, under solvent-free conditions. This reaction proceeds only in the presence of the catalyst because no new product was detected in the absence of this catalyst (see Table 1). The reaction was also studied in different solvents, such as EtOH, CH₃CN, CH₂Cl₂, CHCl₃, and *n*-hexane to compare with the solvent-free conditions. It was found that solvent-free conditions give better results in respect of reaction times and yields (Table 2). The effect of temperature was also checked and based on the obtained results 120 °C was selected for all the examined reactions (see Table 1). The condensation of various amides and aldehydes with 2-naphthol under the optimum conditions was then carried out in the presence of RGO/CoFe₂O₄@Cu(II) as catalyst. In all the examined reactions, aminoalkylnaphthols were found to be the only products and no other by-products were observed.

In this study, it was also found that aromatic aldehydes containing either electron-donating or electron-withdrawing groups give the target product with high yield. However, aromatic aldehydes with electron-donating groups (OH, N(CH₃)₂, CH₃) required longer reaction times compared to those aldehydes bearing electron-withdrawing groups (Cl, NO₂, Br). These ob-

Table 5 Reusability of RGO/CoFe₂O₄@Cu(II) nanocatalyst

Run	Fresh	1	2	3	4	5
Yield (%)	97	96	96	96	95	93

servations are in agreement with the previously reported findings [1–7]. Some of these condensation reactions were performed using urea or benzamide instead of acetamide and a set can be seen in Table 3, longer reaction times were needed for these substrates to give substantial yields.

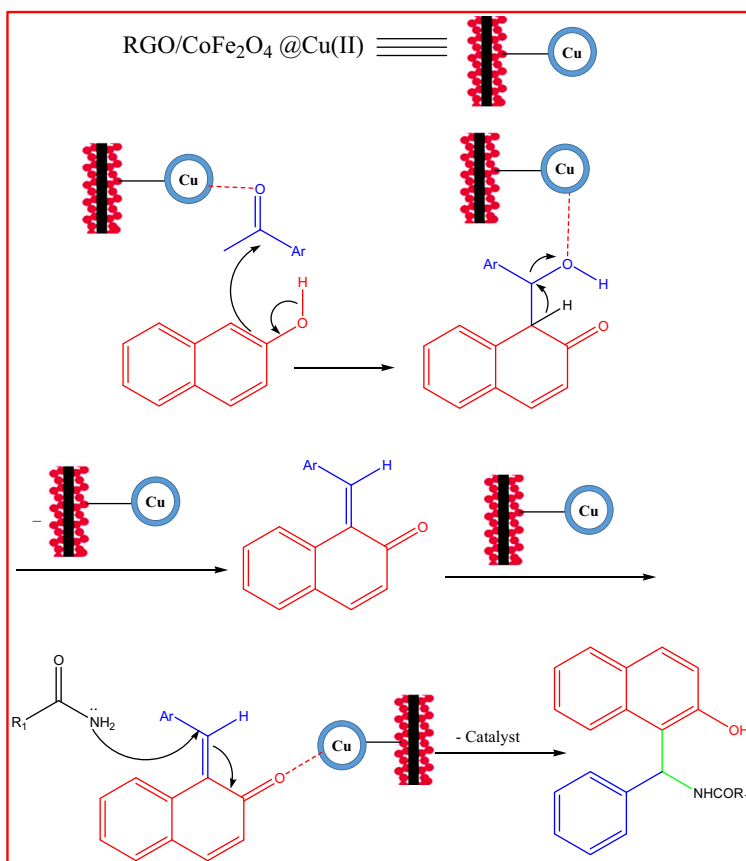
In Table 4, the catalytic activity of the as-prepared nanocatalyst was compared with other recently studied catalysts for the synthesis of amidoalkylnaphthol derivatives. The data show that the catalyst of the present work is superior to the other reported catalysts with respect to reaction times and reaction conditions. The superiority of our introduced nanocatalyst will become more evident when its magnetic property is taken into account which provides a facile and efficient separation for the catalyst in the recycling process.

Recycling and reusability of the catalyst

Facile recovery is considered as an important advantage of the heterogeneous catalysts in organic chemistry and industry. In order to test the as-made

catalyst reusability, the synthesis of amidoalkylnaphthol derivatives was achieved in the presence of catalytic amount of RGO/CoFe₂O₄@Cu(II) under optimized reaction conditions. After completion of the reaction, the catalyst was isolated by applying an external magnetic force, followed by washing it for three times with ethanol. After drying the isolated catalyst at 100 °C for 2 h, it was reused in a new reaction with fresh substrates. The results of reusability tests of this catalyst are presented in Table 5, which indicates the recovered catalyst could be reused for at least five successive times with almost no change in its catalytic performance. The amount of copper was also measured in the recycled nanocatalyst after five runs by ICP-AES analysis. It was found that the copper content of the catalyst remained almost unchanged during the catalytic reactions indicating no detectable leaching of the catalyst into the solution. SEM and TEM images of RGO/CoFe₂O₄@Cu(II), after reusing it for five runs, are presented in Fig. S3, and the PXRD pattern of the same sample is depicted in Fig. S4. These

Fig. 9 Mechanism for the formation of amidoalkyl naphthols catalyzed by RGO/CoFe₂O₄@Cu(II)



analyses clearly revealed that the morphology and the structure of the used catalyst, after five successive catalytic reactions, are almost the same as fresh catalyst.

Mechanism for the catalysis reactions

Based on the previously reported research (Nasr esfahani et al. 2016; Zhang et al. 2010) and our observation, a plausible mechanism for the formation of amidoalkyl naphthols from 2-naphthol, acetamide and aldehyde was proposed which is presented in Fig. 9. According to this mechanism, the copper complex can act as a Lewis acid which activates the carbonyl group of the aldehyde to form intermediate (I). A subsequent nucleophilic attack by 2-naphthol on the latter intermediate will result in the formation of intermediate (II). Finally, a Michael reaction occurs through the addition of amide or urea to the last intermediate will lead to the production of 1-amidoalkyl-2-naphthol derivative product.

Conclusion

In brief, a straightforward and facile procedure was used to immobilize a Cu(II) complex onto magnetized reduced graphene to construct a novel nanocatalyst. This composite was prepared in order to be employed as catalyst for the synthesis of 1-amidoalkyl-2-naphthols using multicomponent condensation reactions. It was shown that the as-synthesized nanocatalyst can efficiently catalyze the condensation of 2-naphthol, aldehydes, and amides to give excellent yields of 1-amidoalkyl-2-naphthol derivatives. According to the obtained results and the reaction conditions, the current catalysis system can be considered as an efficient, rapid, and green procedure for the synthesis of the biologically and pharmaceutically important substituted amidoalkyl naphthols.

Funding information The authors wish to acknowledge the support of this work (grant no. 1396) provided by the Research Council of Shahid Chamran University of Ahvaz, Iran.

Compliance with ethical standards

Conflict of interest The authors declare that they have no conflict of interest.

References

- Allen MJ, Tung VC, Kaner RB (2009) *Chem Rev* 110:132–145
- Cai Z, Shu C, Peng Y (2014) Magnetically recoverable nano-sized mesoporous solid acid: effective catalysts for the synthesis of 1-amidoalkyl-2-naphthols. *Monatsh Chem* 145(10):1681–1687. <https://doi.org/10.1007/s00706-014-1246-1>
- Chandekar KV, Kant KM (2017) Superlattices Microstruct. In press. <https://doi.org/10.1016/j.spmi.2017.07.023>
- Chang CF, Truong QD, Chen JR (2013) RETRACTED: Graphene as excellent support for rapid and efficient near infrared-assisted triptic proteolysis. *Colloid Surf B* 104:221–228. <https://doi.org/10.1016/j.colsurfb.2012.11.040>
- Chen J, Yao B, Li C, Shi G (2013) An improved Hummers method for eco-friendly synthesis of graphene oxide. *Carbon* 64: 225–229. <https://doi.org/10.1016/j.carbon.2013.07.055>
- Dupont J, de Souza RF, PAZ S (2002) Ionic liquid (molten salt) phase organometallic catalysis. *Chem Rev* 102(10):3667–3692. <https://doi.org/10.1021/cr010338r>
- Gemeay AH, El-Halwagy ME, El-Sharkawy RG, Zaki AB (2017) Chelation mode impact of copper(II)-aminosilane complexes immobilized onto graphene oxide as an oxidative catalyst. *J Environ Chem Eng* 5(3):2761–2772. <https://doi.org/10.1016/j.jece.2017.05.020>
- Georgakilas V, Otyepka M, Bourlinos AB, Chandra V, Kim N, Kemp KC, Hobza P, Zboril R, Kim KS (2012) Functionalization of graphene: covalent and non-covalent approaches, derivatives and applications. *Chem Rev* 112(11):6156–6214. <https://doi.org/10.1021/cr3000412>
- Guo J, Li Y, Zhu S, Chen Z, Liu Q, Zhang D, Moon WJ, Song DM (2012) Synthesis of WO₃@Graphene composite for enhanced photocatalytic oxygen evolution from water. *RSC Adv* 2(4):1356–1363. <https://doi.org/10.1039/C1RA00621E>
- Gupta A, Kour D, Gupta VK, Kapoor KK (2016) Graphene oxide mediated solvent-free three component reaction for the synthesis of 1-amidoalkyl-2-naphthols and 1,2-dihydro-1-arylnaphth[1,2-e][1,3]oxazin-3-ones. *Tetrahedron Lett* 57(43):4869–4872. <https://doi.org/10.1016/j.tetlet.2016.09.067>
- Hosseini SH, Asadnia A (2012) Synthesis, characterization, and microwave-absorbing properties of polypyrrole/MnFe₂O₄ nanocomposite. *J Nanomater* 2012:1–6. <https://doi.org/10.1155/2012/198973>
- Jiang WQ, An LT, Zou JP (2008) Molybdophosphoric acid: an efficient Keggin-type heteropolyacid catalyst for the one-pot three-component synthesis of 1-amidoalkyl-2-naphthols. *Chin J Chem* 26(9):1697–1701. <https://doi.org/10.1002/cjoc.200890307>
- Jiang Y, Guo C, Xia H, Mahmood I, Liu C, Liu H (2009) Magnetic nanoparticles supported ionic liquids for lipase immobilization: enzyme activity in catalyzing esterification. *J Mol Catal B* 58(1–4):103–109. <https://doi.org/10.1016/j.molcatb.2008.12.001>
- Kantevari S, Vuppalapati SVN, Nagarapu L (2007) Montmorillonite K10 catalyzed efficient synthesis of amidoalkyl naphthols under solvent free conditions. *Catal Commun* 8(11):1857–1862. <https://doi.org/10.1016/j.catcom.2007.02.022>
- Khabazzadeh H, Saidi K, Seyedi N (2009) Cu-exchanged heteropoly acids as efficient and reusable catalysts for

- preparation of 1-amidoalkyl-2-naphthols. *J Chem Sci* 121(4): 429–434. <https://doi.org/10.1007/s12039-009-0050-7>
- Khairnar BJ, Girase PS, Mane DV, Chaudhari BR (2016) *Der Pharma Chemica* 8:137–141
- Kiasat AR, Mouradzadegan A, Saghanezhad SJ (2013) Poly(4-vinylpyridinium butane sulfonic acid) hydrogen sulfate: an efficient, heterogeneous poly(ionic liquid), solid acid catalyst for the one-pot preparation of 1-amidoalkyl-2-naphthols and substituted quinolines under solvent-free conditions. *Chin J Catal* 34(10):1861–1868. [https://doi.org/10.1016/S1872-2067\(12\)60659-7](https://doi.org/10.1016/S1872-2067(12)60659-7)
- Kumar ER, Jayaprakash R, Kumar TA, Kumar S (2013) Effect of reaction time on particle size and dielectric properties of manganese substituted CoFe_2O_4 nanoparticles. *J Phys Chem Solids* 74(1):110–114. <https://doi.org/10.1016/j.jpms.2012.08.008>
- Lee JH, Huh YM, Jun YW, Seo JW, Jang JT, Song HT, Kim S, Cho EJ, Yoon HG (2007) *Suh JS, Cheon. J Nat Med* 13(1): 95–98. <https://doi.org/10.1038/nm1467>
- Li Z, Wu S, Ding H, Zheng D, Hu J, Wang X, Huo Q, Guan J, Kan Q (2013) Immobilized Cu(II) and Co(II) salen complexes on graphene oxide and their catalytic activity for aerobic epoxidation of styrene. *New J Chem* 37(5):1561–1568. <https://doi.org/10.1039/c3nj00099k>
- Majidi RF, Sanjani NS, Agend F (2006) Encapsulation of magnetic nanoparticles with polystyrene via emulsifier-free miniemulsion polymerization. *Thin Solid Films* 515(1): 368–374. <https://doi.org/10.1016/j.tsf.2005.12.102>
- Maleki B, Sheikh E, Seresht ER, Eshghi H, Ashrafi SS, Khojastehnezhad A, Veisi H (2016) One-pot synthesis of 1-amidoalkyl-2-naphthols catalyzed by polyphosphoric acid supported on silica-coated NiFe_2O_4 nanoparticles. *Org Prep Proc Int* 48(1):37–44. <https://doi.org/10.1080/00304948.2016.1127098>
- Moghani H, Mobinikhaledi A, Blackman AG, Sarough-Farahani E (2014) Sulfanilic acid-functionalized silica-coated magnetite nanoparticles as an efficient, reusable and magnetically separable catalyst for the solvent-free synthesis of 1-amido- and 1-aminoalkyl-2-naphthols. *RSC Adv* 4(54): 28176–28185. <https://doi.org/10.1039/C4RA03676J>
- Nagarapu WL, Baseeruddin M, Apuri S, Kantevari S (2007) Potassium dodecatungstocobaltate trihydrate ($\text{K}_5\text{CoW}_{12}\text{O}_{40}\cdot 3\text{H}_2\text{O}$): A mild and efficient reusable catalyst for the synthesis of amidoalkyl naphthols in solution and under solvent-free conditions. *Catal Commun* 8(11):1729–1731. <https://doi.org/10.1016/j.catcom.2007.02.008>
- Nagawade RR, Shinde DB (2007) Sulphamic acid ($\text{H}_2\text{NSO}_3\text{H}$)-catalyzed multicomponent reaction of β -naphthol: an expeditious synthesis of amidoalkyl naphthols. *Chin J Chem* 25(11):1710–1714. <https://doi.org/10.1002/cjoc.200790316>
- Nandi GC, Samai S, Kumar R, Singh MS (2009) Atom-efficient and environment-friendly multicomponent synthesis of amidoalkyl naphthols catalyzed by P_2O_5 . *Tetrahedron Lett* 50(51):7220–7222. <https://doi.org/10.1016/j.tetlet.2009.10.055>
- Nasr esfahani Z, Kassae MZ, Eidi E (2016) Homopiperazine sulfamic acid functionalized mesoporous silica nanoparticles (MSNs-HPZ-SO₃H) as an efficient catalyst for one-pot synthesis of 1-amidoalkyl-2-naphthols. *New J Chem* 40(5): 4720–4726. <https://doi.org/10.1039/C5NJ02974K>
- Patel RN, Sondhiya VP, Shukla KK, Patel DK, Singh Y (2013) Synthesis, crystal structure, electrochemical and bioactivities of pyridine-2-carboxylato bridged copper(II) complexes. *Polyhedron* 50(1):139–145. <https://doi.org/10.1016/j.poly.2012.10.027>
- Polshettiwar V, Luque R, Fihri A, Zhu H, Bouhrara M, Basset JM (2011) Magnetically recoverable nanocatalysts. *Chem Rev* 111(5):3036–3075. <https://doi.org/10.1021/cr100230z>
- Rakhtshah J, Salehzadeh S (2016) β -cyclodextrin-monosulphonic acid catalyzed efficient synthesis of 1-amidoalkyl-2-naphthols. *Appl Organomet Chem* 31(2):1–9. <https://doi.org/10.1002/aoc.3690>
- Rakumar T, Rao GR (2008) Investigation of hybrid molecular material prepared by ionic liquid and polyoxometalate anion. *J Chem Sci* 120(6):587–594. <https://doi.org/10.1007/s12039-008-0089-x>
- Rayati S, Khodaei E, Shokooi S, Jafarian M, Elmi B, Wojtczak A (2017) Cu-Schiff base complex grafted onto graphene oxide nanocomposite: synthesis, crystal structure, electrochemical properties and catalytic activity in oxidation of olefins. *Inorg Chim Acta* 466:520–528. <https://doi.org/10.1016/j.ica.2017.07.013>
- Rondinone AJ, Samia ACS, Zhang ZJ (1999) Superparamagnetic relaxation and magnetic anisotropy energy distribution in CoFe_2O_4 spinel ferrite nanocrystallites. *J Phys Chem B* 103(33):6876–6880. <https://doi.org/10.1021/jp9912307>
- Safari J, Zarnegar Z (2014) Synthesis of amidoalkyl naphthols by nano- Fe_3O_4 modified carbon nanotubes via a multicomponent strategy in the presence of microwaves. *Ind Eng Chem Res* 20(4):2292–2297. <https://doi.org/10.1016/j.jiec.2013.10.004>
- Sahoo B, Devi KSP, Kumar Sahu S, Nayak S, Maiti TK, Dhara D, Pramanik P (2013) Facile preparation of multifunctional hollow silica nanoparticles and their cancer specific targeting effect. *Biomater Sci* 1(6):647–657. <https://doi.org/10.1039/c3bm00007a>
- Selvam NP, Perumal PT (2006) A new synthesis of acetamidophenols promoted by $\text{Ce}(\text{SO}_4)_2$. *Tetrahedron Lett* 47(42): 7481–7484. <https://doi.org/10.1016/j.tetlet.2006.08.038>
- Shaterian HR, Yarahmadi H (2008) A modified reaction for the preparation of amidoalkyl naphthols. *Tetrahedron Lett* 49(8): 1297–1300. <https://doi.org/10.1016/j.tetlet.2007.12.093>
- Shaterian HR, Hosseini A, Yarahmadi H, Ghashang M (2008a) Alumina sulfuric acid: an efficient heterogeneous catalyst for the synthesis of amidoalkyl naphthols. *Lett Org Chem* 5(4): 290–295. <https://doi.org/10.2174/157017808784049524>
- Shaterian HR, Yarahmadi H, Ghashang M (2008b) An efficient, simple and expeditious synthesis of 1-amidoalkyl-2-naphthols as ‘drug like’ molecules for biological screening. *Bioorg Med Chem Lett* 18(2):788–792. <https://doi.org/10.1016/j.bmcl.2007.11.035>
- Sheshmani S, Amini R (2013) *Carbohydr Polym* 95:348–359
- Singha RK, Balaa R, Duvedia R, Kumar S (2015) *Iran J Catal* 5: 187–206
- Sofia LTA, Krishnan A, Sankar M, Kala Raj NK, Manikandan P, Rajamohanam PR, Ajithkumar TG (2009) Immobilization of phosphotungstic acid (PTA) on imidazole functionalized silica: evidence for the nature of PTA binding by solid state NMR and reaction studies. *J Phys Chem C* 113(50):21114–21122. <https://doi.org/10.1021/jp906108e>

- Su DS, Perathoner S, Centi G (2013) Nanocarbons for the development of advanced catalysts. *Chem Rev* 113(8):5782–5816. <https://doi.org/10.1021/cr300367d>
- Taghrir H, Ghashang M, Bireghan MN (2016) Preparation of 1-amidoalkyl-2-naphthol derivatives using barium phosphate nano-powders. *Chin Chem Lett* 27(1):119–126. <https://doi.org/10.1016/j.cclet.2015.08.011>
- Tang Y, Huang F, Zhao W, Liu Z, Wan D (2012) Synthesis of graphene-supported $\text{Li}_4\text{Ti}_5\text{O}_{12}$ nanosheets for high rate battery application. *J Mater Chem* 22(22):11257–11260. <https://doi.org/10.1039/c2jm30624g>
- Tayebee R, Amini MM, Rostamian H, Aliakbari A (2014) Preparation and characterization of a novel Wells–Dawson heteropolyacid-based magnetic inorganic–organic nanohybrid catalyst $\text{H}_6\text{P}_2\text{W}_{18}\text{O}_{62}/\text{pyridino-Fe}_3\text{O}_4$ for the efficient synthesis of 1-amidoalkyl-2-naphthols under solvent-free conditions. *Dalton Trans* 43(4):1550–1563. <https://doi.org/10.1039/C3DT51594J>
- Virtanen P, Salmi TO, Mikkola JP (2010) Supported ionic liquid catalysts (SILCA) for preparation of organic chemicals. *Top Catal* 53(15–18):1096–1103. <https://doi.org/10.1007/s11244-010-9540-6>
- Xiong P, Hu G, Fan Y, Zhang W, Zhu J, Wang X (2014) Ternary manganese ferrite/graphene/polyaniline nanostructure with enhanced electrochemical capacitance performance. *J Power Sources* 266:384–392. <https://doi.org/10.1016/j.jpowsour.2014.05.048>
- Yan X, Chen J, Xue Q, Miele P (2010) Synthesis and magnetic properties of CoFe_2O_4 nanoparticles confined within mesoporous silica. *Microporous Mesoporous Mater* 135(1–3):137–142. <https://doi.org/10.1016/j.micromeso.2010.07.001>
- Zhang Y, Zhao Y, Xia C (2009) Basic ionic liquids supported on hydroxyapatite-encapsulated $\gamma\text{-Fe}_2\text{O}_3$ nanocrystallites: an efficient magnetic and recyclable heterogeneous catalyst for aqueous Knoevenagel condensation. *J Mol Catal A* 306(1–2):107–112. <https://doi.org/10.1016/j.molcata.2009.02.032>
- Zhang Q, Luo J, Wei Y (2010) A silica gel supported dual acidic ionic liquid: an efficient and recyclable heterogeneous catalyst for the one-pot synthesis of amidoalkyl naphthols. *Green Chem* 12(12):2246–2254. <https://doi.org/10.1039/c0gc00472c>
- Zheng X, Luo S, Zhang L, Cheng JP (2009) *Green Chem* 1:455–458
- Zhu X, Lee YR, Kim SH (2012) Facile one-pot synthesis of 1-amidoalkyl-2-naphthols by $\text{RuCl}_2(\text{PPh}_3)_3$ -catalyzed multi-component reactions. *Bull Kor Chem Soc* 33(8):2799–2802. <https://doi.org/10.5012/bkcs.2012.33.8.2799>